INSTITUTE OF FLUID-FLOW MACHINERY
POLISH ACADEMY OF SCIENCES

TRANSACTIONS OF THE INSTITUTE OF FLUID-FLOW MACHINERY

112

GDAŃSK 2003

TRANSACTIONS OF THE INSTITUTE OF FLUID-FLOW MACHINERY

Appears since 1960

Aims and Scope

Transactions of the Institute of Fluid-Flow Machinery have primarily been established to publish papers from four disciplines represented at the Institute of Fluid-Flow Machinery of Polish Academy of Sciences, such as:

- Liquid flows in hydraulic machinery including exploitation problems,
- Gas and liquid flows with heat transport, particularly two-phase flows,
- Various aspects of development of plasma and laser engineering,
- Solid mechanics, machine mechanics including exploitation problems.

The periodical, where originally were published papers describing the research conducted at the Institute, has now appeared to be the place for publication of works by authors both from Poland and abroad. A traditional scope of topics has been preserved.

Only original and written in English works are published, which represent both theoretical and applied sciences. All papers are reviewed by two independent referees.

EDITORIAL AND PUBLISHING OFFICE

IFFM Publishers (Wydawnictwo IMP), Institute of Fluid Flow Machinery, Fiszera 14, 80-952 Gdańsk, Poland, Tel.: +48(58)3411271 ext. 141, Fax: +48(58)3416144, E-mail: esli@imp.gda.pl

Financial support of publication of this journal is provided by the State Committee for Scientific Research, Warsaw, Poland

Terms of subscription

Subscription order and payment should be directly sent to the Publishing Office

Warunki prenumeraty w Polsce

Wydawnictwo ukazuje się przeciętnie dwa lub trzy razy w roku. Cena numeru wynosi 20,- zł + 5,- zł koszty wysyłki. Zamówienia z określeniem okresu prenumeraty, nazwiskiem i adresem odbiorcy należy kierować bezpośrednio do Wydawcy (Wydawnictwo IMP, Instytut Maszyn Przepływowych PAN, ul. Gen. Fiszera 14, 80-952 Gdańsk). Osiągalne są również wydania poprzednie. Prenumerata jest również realizowana przez jednostki kolportażowe RUCH S.A. właściwe dla miejsca zamieszkania lub siedziby prenumeratora. W takim przypadku dostawa następuje w uzgodniony sposób.

ISSN 0079-3205

TRANSACTIONS OF THE INSTITUTE OF FLUID-FLOW MACHINERY

No. 112, 2003, 103-118

ROBERT PASTUSZKO*

Temperature field in two-layer fins immersed in boiling water

Kielce University of Technology, Chair of Thermodynamics and Fluid Mechanics, Al. Tysiąclecia P.P. 7, PL - 25-314 Kielce, Poland

Abstract

The steady, two-dimensional temperature field for a two-layer fin, composed of copper core and porous covering, filled with boiling water was calculated. Simplified one-dimensional model was also presented. Fin parameters were: height – 10 mm, thickness – 3 mm, porosity – 60 %, capillary-porous structure (CPS) layer thickness – 0.6 mm. The modified finite difference method was described. The heat transfer coefficient was assumed to vary with a power-law-type formula. Temperature distribution in the fin vertical section was determined experimentally with a thermovision camera. A reasonable degree of congruence was found to exist between the theoretical and the experimental results.

Keywords: Two-layer fins; Porous structure; Nucleate boiling

Nomenclature

c	– constant	R	– thermal resistance, K/W
CPS	– capillary-porous structure	s	– space between fins, mm
d	– pore diameter, mm	T	– temperature, K
g	– thickness, m/s^2	w	– fin width, mm
g	– gravity , mm	x	– coordinate
h	– fin height, mm	y	– coordinate
i	– index count of grid lines in x direction	α	– heat transfer coefficient, W/m^{2}K
		δ	– thickness, mm
j	– index count of grid lines in y direction	Δx	– node distance in x direction
		Δy	– node distance in y direction
m	– fin parameter, m^{-1}	ΔT	– excess temperature, K
N	– number of fins	Θ	– excess temperature, K

*E-mail address: tmprp@tu.kielce.pl

Q	–	heat transfer rate, W	λ	–	thermal conductivity, W/mK
q	–	heat flux density, W/m^2	Π	–	porosity
p	–	perimeter, m			

Subscripts

b	–	base	Cu	–	copper (core)
e	–	effective	if	–	inter-fin
l	–	liquid	m	–	mean
n	–	exponent	por	–	porous layer
sat	–	saturation	sk	–	skeleton
N	–	direction (north)	S	–	direction (south)
E	–	direction (east)	W	–	direction (west)

1 Introduction

The application of a two-layer fin composed of a copper core covered with a capillary-porous layer, made of sintered copper wires, leads to a significant increase in the transferred heat flux and heat transfer coefficients in the whole range of nucleate boiling for water, ethanol and freon 113 [1]. An attempt was made to determine experimentally the temperature distribution in a two-layer fin, which was compared with numerical calculations. Thermovision camera was used to determine isotherms in the fin vertical section. The special set-up allowed the measurement of temperature field on one isolated fin side surface, which did not come in contact with boiling water.

2 Experimental set-up

The diagram of the experimental set-up for the determination of boiling curves and temperature distribution in the fin section was presented in Fig.1.

In order to measure the temperature distributions along the fin with a thermovision camera, it was necessary to make a special module (Fig. 2), being a modified version of the basic module for determination of boiling curves (described in section 2). The most important change was the application of textile laminate sleeve, Fig. 2 (1), between the finned sample (2) and teflon separator (6). The fin and sleeve contact surface was sealed with an adhesive layer. The solution presented above offers the possibility of thermal radiation intensity measurement on the external surface of the fin section. The fin profile surface was additionally covered with a thin adhesive layer which limited heat losses and prevented the liquid leakage out of the porous layer.

The best thermographs were obtained by covering the open side of the fin with a thin layer of cement (0.5 mm).

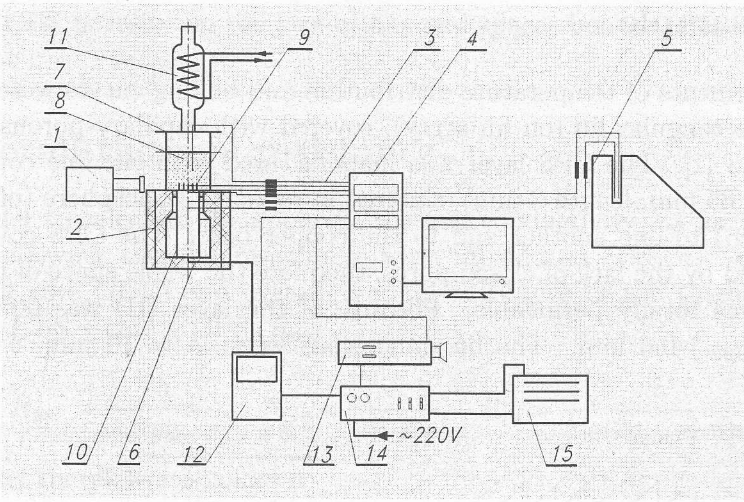

Figure 1. Temperature measurement and power supply system: 1 – IR camera; 2 – teflon casing; 3 – compensating leads; 4 computer with APCI-3200 board; 5 – ice point reference cell; 6 – insulation; 7 – glass vessel; 8 – boiling liquid; 9 – investigated sample; 10 – copper bar with cartridge heater; 11 – condenser; 12 – wattmeter; 13 – temperature excess signalling module; 14 – fuses and the power shutting off system, controlled by the signal from (13); 15 – autotransformer.

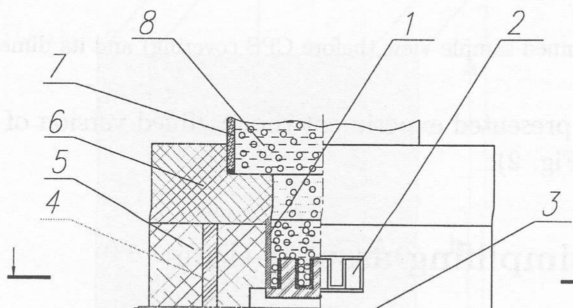

Figure 2. Elements of the module for thermovision investigation: 1 – textile laminate sleeve, 2 – fin with capillary-porous covering, 3 – heating cylinder, 4 – ceramic sleeve, 5 – insulation, 6 – teflon separator, 7 – glass vessel, 8 – boiling liquid.

3 Fin sample

Measurements of temperature distribution and boiling curves were taken fo a vertical rectangular fin (on fin array), covered with capillary-porous structu (CPS), Fig.3 [1]. The CPS layer was manufactured with cut fine copper wire (diameter 0.05 mm, length 3 mm), sintered in reducing atmosphere (of hydrog and nitrogen) to one another and to the copper base. The CPS covering wa characterised by the lack of closed pores, therefore the whole space of the porou structure was totally permeable. Porosity of the layer (Π) was 60%, and n thickness (g_{por}) 0.6 mm. The fin dimensions were: h = 10 mm, δ = 3 mm s = 5 mm.

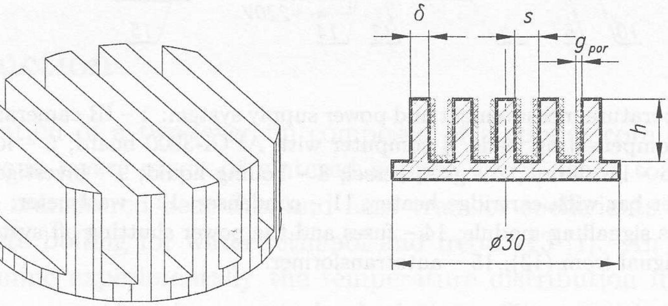

Figure 3. Finned sample view (before CPS covering) and its dimensions.

However in the presented experiment the modified version of the above bas module was used (Fig. 2).

4 General simplifing assumptions

General simplifying assumptions with respect to one- and two-dimensi heat conduction in a fin are to be found in literature [1-5]:

- the thermal properties of the core and CPS layer (specific heat, condu vity) are constant,
- there is no heat source in the fin,
- the temperature of the surrounding boiling fluid is constant and equ saturation temperature T_{sat},
- the base temperature is uniform,
- the core and CPS layer materials are homogeneous
- fin thickness (δ) and CPS thickness (g_{por}) are constant,

- the CPS porosity on the face of fins and spaces between fins remains constant

5 Overall thermal resistance

In order to calculate the apparent thermal conductivity λ_m for a compound fin, the following thermal resistances were introduced (Fig. 4): porous layer (R_{por}), fin core (R_{Cu}) and overall thermal resistance of the three layer sandwich, e.g. CPS + core + CPS (R_m):

$$R_{por} = \frac{h}{\lambda_e 2 g_{por} w}, \quad R_{Cu} = \frac{h}{\lambda_{Cu} \delta w}, \quad R_m = \frac{h}{\lambda_m (2g_{por} + \delta) w}. \tag{1}$$

For parallel thermal resistances:

$$\frac{1}{R_m} = \frac{1}{R_{por}} + \frac{1}{R_{Cu}}. \tag{2}$$

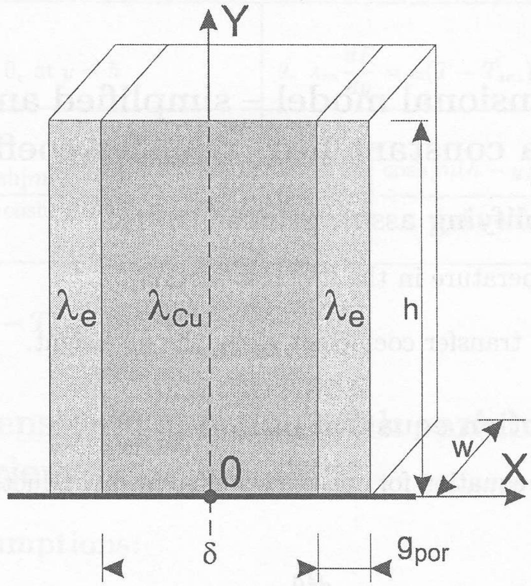

Figure 4. Fin vertical section – coordinate system for two-dimensional analysis.

The dependence for apparent thermal conductivity for the core and the porous layer, obtained from Eqs. (1) and (2), takes the form:

$$\lambda_m = \frac{\lambda_{Cu}\delta + 2\lambda_e g_{por}}{\delta + 2g_{por}}. \tag{3}$$

Effective capillary-porous covering thermal conductivity is obtained as follows

$$\lambda_e = \Pi \lambda_l + \lambda_{sk}$$

and skeleton thermal conductivity can be expressed from the chart shown Fig. 5.

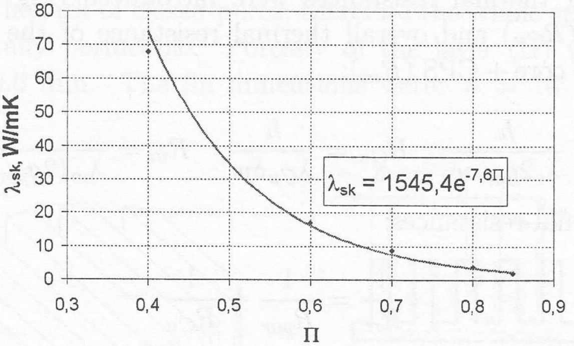

Figure 5. Dependence of skeleton thermal conductivity on CPS porosity.

6 One-dimensional model – simplified analitycal solutions for a constant heat transfer coefficient

Additional simplifying assumptions:

- constant temperature in the fin cross-section,
- constant heat transfer coefficient along the fin height.

Thermal conduction equation

The differential equation for one dimensional heat conduction in a rectangular fin is:

$$\frac{d^2\theta}{dy^2} = m^2\theta$$

where: $\theta = T - T_{sat}$, $m^2 = \dfrac{\alpha\, p}{\lambda F}$.
Assuming $\delta + 2_{por} << w$, we obtain:

$$m^2 = \frac{2\alpha}{\lambda\,\delta}$$

For a fin covered with a capillary-porous layer of g_{por} thickness, the formula (6) takes the following form:

$$m^2 = \frac{2\alpha}{\lambda_m(\delta + 2g_{por})}. \tag{7}$$

Boundary conditions and solutions for insulated and not insulated fin tip

Table 1 presents the boundary conditions and temperature distributions for a very well known analytical solution.

Table 1. Boundary conditions and temperature distribution for 1D model

insulated fin tip – without heat transfer through the tip	not insulated fin tip – heat transfer through the tip
1. $T = T_b$, at $y = 0$,	1. $T = T_b$, at $y = 0$,
2. $\frac{dT}{dy} = 0$, at $y = h$	2. $\lambda_m \frac{dT}{dy} = \alpha(T - T_{sat})$, at $y = h$
$\Theta = \Theta_b \frac{\cosh[m(h-y)]}{\cosh(mh)}$	$\Theta = \Theta_b \left[\frac{\cosh[m(h-y)] - \frac{\alpha}{mh}\sinh[m(h-y)]}{\cosh(mh) + \frac{\alpha}{m\lambda_m}\sinh(mh)} \right]$

where: $\theta_b = T_b - T_{sat}$

7 Two-dimensional solution with variable heat transfer coefficient

Additional assumptions:

- variable local heat transfer coefficient along the fin is specified by the dependence: $\alpha = C(T - T_{sat})^{n-1}$, where T denoted local temperature along the fin height (y),
- at the fin end, on its frontal surface, heat is transferred by convection,
- two-dimensional, steady state of conduction.

Determination of thermal conductivity

Depending on the horizontal coordinate (x), thermal conductivity of fin with CPS layer assumed the following values:

$$\lambda = \begin{cases} \lambda_{Cu} & \text{at} \quad 0 \leq x < \frac{\delta}{2}, \\ \lambda_m & \text{at} \quad x = \frac{\delta}{2}, \\ \lambda_e & \text{at} \quad \frac{\delta}{2} < x \leq \frac{\delta}{2} + g_{por}. \end{cases}$$

Determination of C and n constants

Data for nucleate pool boiling for fins with CPS covering were reported in [1]. power law correlation for heat flux density derived from these data has the form

$$q = C\Delta T^n$$

where $n = 1.3 \ldots 1.5$ for boiling water (CPS parameters: $\Pi = 60\%$, $g_{por} =$ 0.6 mm). Value of C was calculated for measured heat flux and superheating the base of fins.

Boundary conditions

Boundary conditions are presented below (Table 2). Figs. 4 and 6 show the coordinate system for two-dimensional heat conduction in the fin with porous covering.

Table 2. Insulated fin tip – without heat transfer through the tip

x	y	
$0 \leq x \leq \frac{\delta}{2} + g_{por}$	0	$T = T_b$
	h	$-\lambda \frac{\partial T}{\partial y} = \alpha(T - T_{sat})$
0	$0 \leq y \leq h$	$\frac{\partial T}{\partial x} = 0$
$\frac{\delta}{2} + g_{por}$		$-\lambda \frac{\partial T}{\partial x} = \alpha(T - T_{sat})$

Numerical solution (control volume method [6])

The steady, two-dimensional temperature field in the fin is described by the Laplace equation together with the corresponding boundary conditions:

$$\frac{\partial^2 T}{\partial x^2} + \frac{\partial^2 T}{\partial y^2} = 0. \tag{10}$$

The modified finite difference numerical method was applied. The Laplace equation was replaced with analogous equations of energy conservation for each identified control volume around the node (i, j), while taking into account the variability of heat transfer coefficient α along the fin [1-3]. In order to construct heat balance equations, seven characteristic nodes along the fin vertical height were chosen (Figs. 6 and 7). Q_N, Q_S, Q_E, Q_W denote heat transfer rates transferred to the closed thermodynamic system from four directions. When the control volumes ($\Delta V = \Delta x \Delta y w$) are small enough, each temperature gradient is approximately equal to the temperature difference between two nodes in contact, divided by the distance between these nodes.

For the control volume ΔV (closed system) under steady state conditions without internal heat sources we have:

$$Q_N + Q_S + Q_E + Q_W = 0. \tag{11}$$

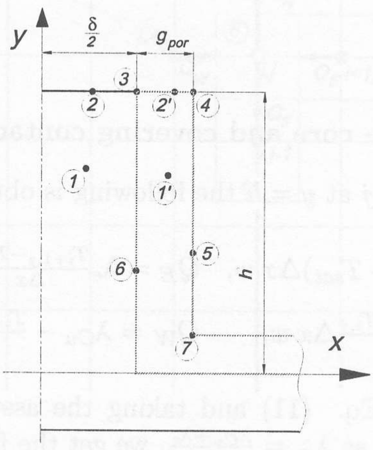

Figure 6. Location of nodes.

8 Heat balance equations and temperature calculations at individual nodes

Index i is used in the range of x coordinate and index j is used in the range of y coordinate.

Internal node – core of fin (1), porous covering (1′), (Figs. 6, 7)

For i at $0 \le x < \frac{\delta}{2} + g_{por}$, and at $x \neq \frac{\delta}{2}$, and for j at $0 \le y < h$ the following is obtained:

$$Q_N = \lambda \frac{T_{i,j+1} - T_{i,j}}{\Delta y} \Delta x\, w, \quad Q_E = \lambda \frac{T_{i+1,j} - T_{i,j}}{\Delta x} \Delta y\, w,$$

$$Q_S = \lambda \frac{T_{i,j-1} - T_{i,j}}{\Delta y} \Delta x\, w, \quad Q_W = \lambda \frac{T_{i-1,j} - T_{i,j}}{\Delta y} \Delta y\, w.$$

where

$$\lambda = \begin{cases} \lambda_{cu}, & \text{for} \quad x < \frac{\delta}{2} \quad (1) \\ \lambda_e, & \text{for} \quad x > \frac{\delta}{2} \quad (1') \end{cases} \quad \text{and } \lambda_e = \Pi \lambda_l + \lambda_{sk} \text{ (from the Eq. 4)}$$

After substitution of the above formula into (11) and taking the assumption $\Delta x = \Delta y$, the temperature in the node equals to:

$$T_{i,j} = \frac{1}{4}(T_{i-1,j} + T_{i+1,j} + T_{i,j-1} + T_{i,j+1}).$$

Frontal surface node – core and covering contact (3), (Figs. 6, 7)

For i at $x = \delta/2$ and for j at $y = h$ the following is obtained:

$$Q_N = -\alpha(T_{i,j} - T_{sat}) \Delta x\, w, \quad Q_E = \lambda_e \frac{T_{i+1,j} - T_{i,j}}{\Delta x} \frac{\Delta y}{2}\, w,$$

$$Q_S = \lambda_m \frac{T_{i,j-1} - T_{i,j}}{\Delta y} \Delta x\, w, \quad Q_W = \lambda_{Cu} - \frac{T_{i-1,j} - T_{i,j}}{\Delta x} \frac{\Delta y}{2} w.$$

After substitution into Eq. (11) and taking the assumption $\Delta x = \Delta y$, $\alpha = C(T_{i,j} - T_{sat})^{n-1}$ as well as $\lambda_m = \frac{\lambda_{Cu} + \lambda_e}{2}$, we get the following equation:

$$2C(T_{i,j} - T_{sat})^n \Delta x + 2(\lambda_e + \lambda_{Cu}) T_{i,j} = \lambda_{Cu}(T_{i-1,j} + T_{i,j-1}) + \lambda_e(T_{i+1,j} + T_{i,j-1})$$

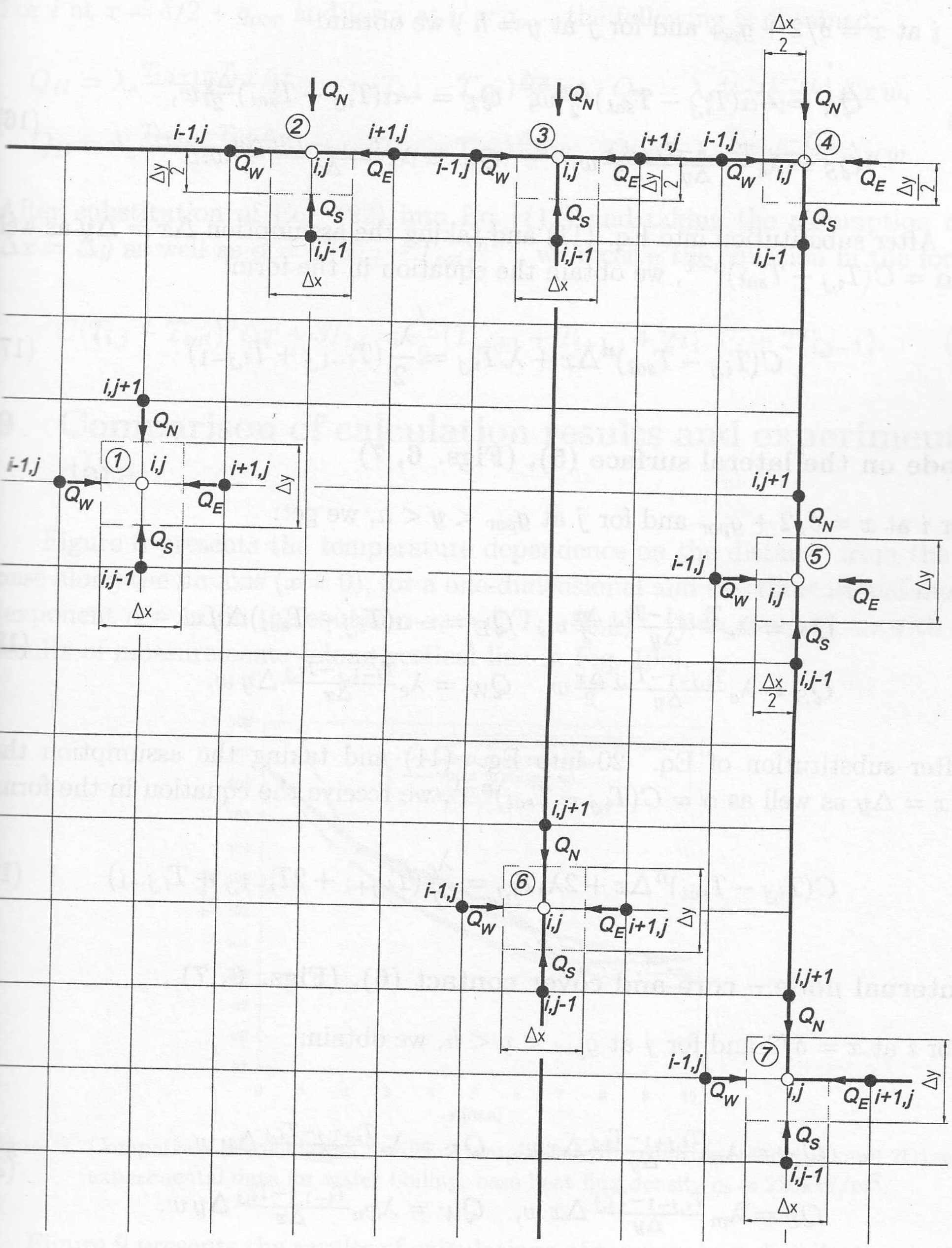

Figure 7. Seven characteristic nodes in the two-layer fin section.

Corner node (4), (Figs. 6, 7)

For i at $x = \delta/2 + g_{por}$ and for j at $y = h$, we obtain:

$$Q_N = -\alpha(T_{i,j} - T_{sat})\tfrac{\Delta x}{2}w, \quad Q_E = -\alpha(T_{i,j} - T_{sat})\tfrac{\Delta y}{2}w,$$

$$Q_S = \lambda_e \tfrac{T_{i,j-1} - T_{i,j}}{\Delta y}\tfrac{\Delta x}{2}w, \qquad Q_W = \lambda_e \tfrac{T_{i-1,j} - T_{i,j}}{\Delta x}\tfrac{\Delta y}{2}w.$$

After substitution into Eq. (11) and taking the assumption $\Delta x = \Delta y$ as well as $\alpha = C(T_{i,j} - T_{sat})^{n-1}$, we obtain the equation in the form:

$$C(T_{i,j} - T_{sat})^n \Delta x + \lambda_e T_{i,j} = \frac{\lambda_e}{2}(T_{i-1,j} + T_{i,j-1})$$

Node on the lateral surface (5), (Figs. 6, 7)

For i at $x = \delta/2 + g_{por}$ and for j at $g_{por} < y < h$, we get:

$$Q_N = \lambda_e \tfrac{T_{i,j+1} - T_{i,j}}{\Delta y}\tfrac{\Delta x}{2}w, \quad Q_E = -\alpha(T_{i,j} - T_{sat})\Delta y\, w,$$

$$Q_S = \lambda_e \tfrac{T_{i,j-1} - T_{i,j}}{\Delta y}\tfrac{\Delta x}{2}w, \quad Q_W = \lambda_e \tfrac{T_{i-1,j} - T_{i,j}}{\Delta x}\Delta y\, w.$$

After substitution of Eq. 20 into Eg. (11) and taking the assumption for $\Delta x = \Delta y$ as well as $\alpha = C(T_{i,j} - T_{sat})^{n-1}$, we receive the equation in the form

$$C(T_{i,j} - T_{sat})^n \Delta x + 2\lambda_e T_{i,j} = \frac{\lambda_e}{2}(T_{i,j+1} + 2T_{i-1,j} + T_{i,j-1})$$

Internal node – core and cover contact (6), (Figs. 6, 7)

For i at $x = \delta/2$ and for j at $g_{por} < y < h$, we obtain:

$$Q_N = \lambda_m \tfrac{T_{i,j+1} - T_{i,j}}{\Delta y}\Delta x\, w, \quad Q_E = \lambda_e \tfrac{T_{i+1,j} - T_{i,j}}{\Delta x}\Delta y\, w,$$

$$Q_S = \lambda_m \tfrac{T_{i,j-1} - T_{i,j}}{\Delta y}\Delta x\, w, \quad Q_W = \lambda_{Cu} \tfrac{T_{i-1,j} - T_{i,j}}{\Delta x}\Delta y\, w.$$

After substitution into (11) and taking the assumption $\Delta x = \Delta y$ as well as $\lambda_m = \frac{\lambda_{Cu} + \lambda_e}{2}$, we come to:

$$(2\lambda_m + \lambda_e + \lambda_{Cu})T_{i,j} = \lambda_m(T_{i,j+1} + T_{i,j-1}) + \lambda_e T_{i+1,j} + \lambda_{Cu} T_{i-1,j}$$

Internal corner (7), (Figs. 6, 7)

For i at $x = \delta/2 + g_{por}$ and for j at $y = g_{por}$, the following is obtained:

$$\begin{aligned} Q_N &= \lambda_e \tfrac{T_{i,j+1}-T_{i,j}}{\Delta y}\tfrac{\Delta x}{2} w - \alpha(T_{i,j}-T_{sat})\tfrac{\Delta x}{2} w, \quad Q_S = \lambda_e \tfrac{T_{i,j-1}-T_{i,j}}{\Delta y}\Delta x\, w, \\ Q_E &= \lambda_e \tfrac{T_{i+1,j}-T_{i,j}}{\Delta x}\tfrac{\Delta y}{2} w - \alpha(T_{i,j}-T_{sat})\tfrac{\Delta y}{2} w, \quad Q_W = \lambda_e \tfrac{T_{i-1,j}-T_{i,j}}{\Delta x}\Delta y\, w. \end{aligned} \tag{22}$$

After substitution of Eq. (22) into Eq. (11) and taking the assumption that $\Delta x = \Delta y$ as well as $\alpha = C(T_{i,j} - T_{sat})^{n-1}$, we receive the equation in the form:

$$C(T_{i,j} - T_{sat})^n \Delta x + 3T_{i,j} = \frac{\lambda_e}{2}(T_{i,j+1} + T_{i+1,j} + 2T_{i-1,j} + 2T_{i,j-1}). \tag{23}$$

9 Comparison of calculation results and experimental data

Figure 8 presents the temperature dependence on the distance from the fin base along the fin axis ($x = 0$), for a one-dimensional and two-dimensional model (exponent $n = 1.3$ in the equation $\alpha_i = C(T_i - T_{sat})^{n-1}$), in comparison with the results of measurements (along vertical line in Fig. 10c).

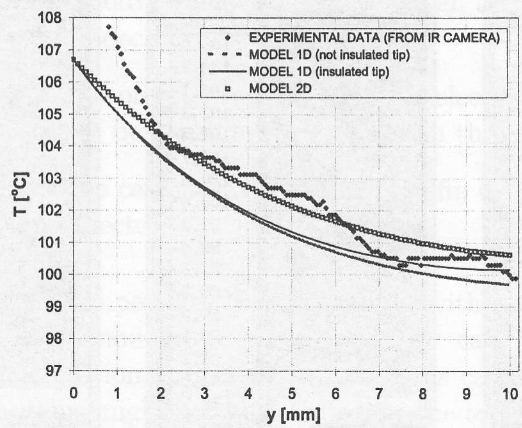

Figure 8. Comparison of calculation results of temperature distribution (model 1D and 2D) with experimental data for water boiling, base heat flux density $q_b \approx 220\text{kW/m}^2$.

Figure 9 presents the results of calculations of temperature distribution in the fin in accordance with the two-dimensional model for the heat flux density at fin base $q_b \approx 220\ \text{kW/m}^2$. Figure 10 shows three thermographs: left for the extreme fin, middle and right – for the centre fin.

For the sake of calculations, it was assumed that the node distance is $\Delta x =$

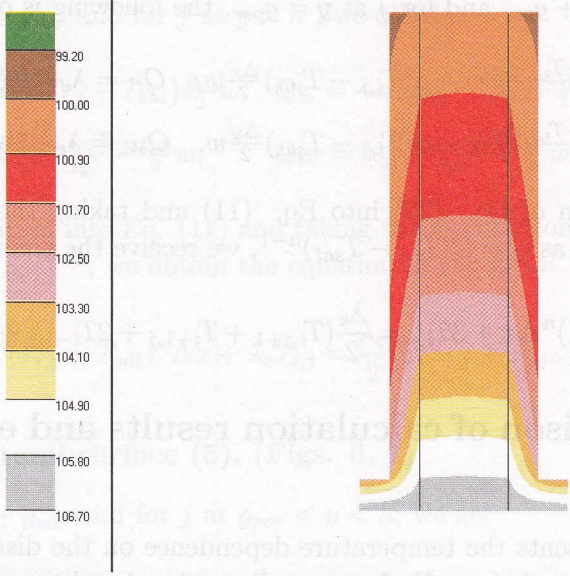

Figure 9. Calculated temperature distributions for boiling of water on the fin surface with porous covering, two-dimensional model, $n = 1.3$, $C = 14500$ (without correction

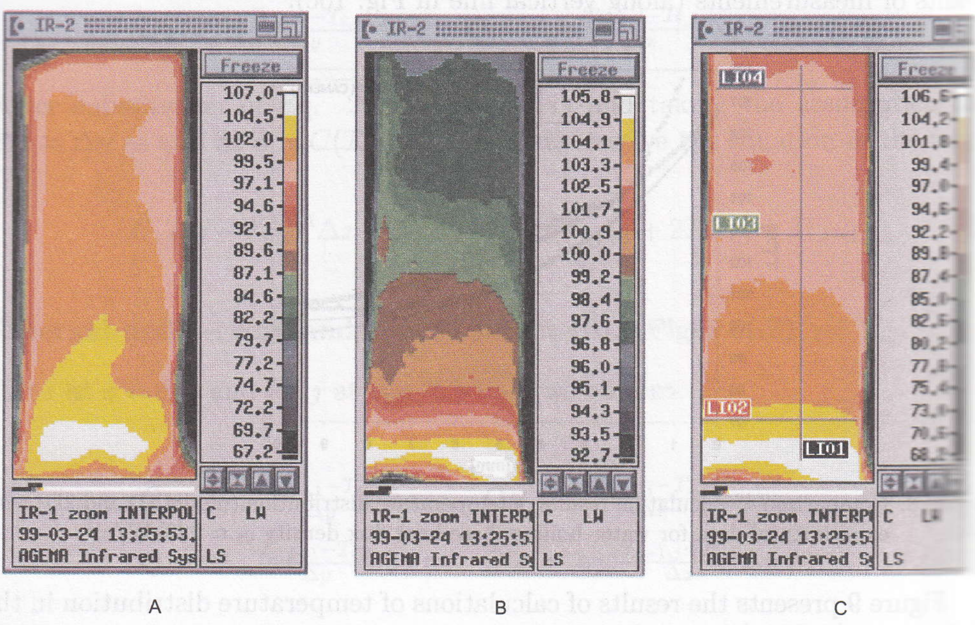

A B C

Figure 10. Examples of thermographs (without correction) for boiling of water on the fin surf with a porous covering, base heat flux density $q_b = 220\ \mathrm{kW/m^2}$; A. extreme fin centre fin – isotherms differences 0.8°C, C. centre fin – isotherms differences

$\Delta y = 0.1$ mm, number of iterations: 50000. The corrected temperature distribution given in the Fig. 8 takes into account the covering of the exposed fin profile with a thin layer of cement. The thermovision camera was calibrated with reference to the temperature at 2 mm from the base, determined due to thermocouple reading extrapolation.

The following thermal parameters: $\lambda_{Cu} = 380$ W/mK, $\lambda_l = 0.68$ W/mK, $\lambda_{sk} = 17$ W/mK, $T_b = 106.7°$C, $C = 14500$, $n = 1.3$ were introduced into the calculation procedure for the fin transferring heat to boiling water.

It can be assumed that the differences between calculated temperature (model 2D) and the experimental data, at $y > 2$ mm, do not exceed the thermocouple reading error limit (approx. 1 K). The largest temperature differences between this model and the experimental data, at $y < 2$ mm, exceed ≈ 2 K.

Temperature distribution measurements in the fin, which transfers heat to the boiling liquid, is based on the assumption that the temperature field in the lateral fin corresponds to the temperature field inside the fin, of the section $h \times \delta$. The hypothesis can be regarded correct at the following assumptions:

- one- or two-dimensional temperature distribution can be assumed for a fin, therefore, temperature fields are the same in the subsequent sections $h \times \delta$ in the fin width,
- heat losses due to convection and radiation from the exposed fin surface are small so can be neglected,
- it is possible to ignore the influence of the sleeve (no. 1, Fig. 2), which reduces the area of boiling liquid contact with the fin lateral surface,
- the thickness of the cement layer spread over fin exposed profile is so small that it can be neglected.

The accuracy of temperature measurements with AGEMA series 900 LW thermovision camera amounts to 1 K. The error can be reduced to 0.25 K when additional calibration with a thermocouple is carried out, yet the above-mentioned assumptions might not be satisfied, so the temperature determination error is estimated to be 1 K.

The accuracy of computation with a numerical method depends mainly on the proper selection of constant C and index n in Eq. (9). Temperature computation error as regards this method is estimated to be 0.2 K.

If the results of temperature distribution measurements are assumed to be reliable, the divergence from numerical computation results might result from a different (more complex) distribution of heat transfer coefficient along the fin height than the one applied to computation.

10 Conclusions

- Application of the temperature dependent heat transfer coefficient to the two-dimensional numerical solution allows more accurate determination of the temperature field in a two-layer fin releasing heat to the boiling liquid.
- Calculation accuracy depends on the correct determination of the constant C and exponent n in the relation describing the boiling curve $q = C\Delta T^n$
- Due to the fact that one side (surface) of the fin does not have contact with the boiling liquid, an additional correction to the temperature field determined with the thermovision camera is required.

Acknowledgements The work was carried out as a part of the grant (KBN 8 T10B 042 20) and research work of Kielce Univ. of Technology No.1.31/8.62

Received 23 October 2002.

References

[1] Pastuszko R.: *Analysis of Boiling Heat Transfer on Finned Surfaces with Capillary-Porous Covering*, Ph.D. thesis, Kielce Univ. of Technology, 1999, (in Polish)

[2] Kern D. Q., Kraus A. D.: *Extended Surface Heat Transfer,* McGraw-Hill, 1972.

[3] Sunden B. and Heggs P. J. (Eds.):, *Recent Advances in Analysis of Heat Transfer for Fin Type Surfaces,* WIT Press, 2000.

[4] Chung B. T. F., Iyer J. R.: *Optimum design of longitudinal rectangular fins and cylindrical spines with variable heat transfer coefficient*, Heat Transfer Engineering, Vol. 14(1993), 31-42.

[5] Liaw S. P., Yeh R. H., *Fins with Temperature Dependent Surface Heat Flux – I Single Heat Transfer Mode*, Int. J. Heat Mass Transfer, Vol. 37(1994), 1509-1515.

[6] Ketkar S. P.: *Numerical Thermal Analysis*, ASME Press, New York 1999.